

## Article

# Factors That Control the Reservoir Quality of the Carboniferous–Permian Tight Sandstones in the Shilouan Block, Ordos Basin

Jing Wang<sup>1,2</sup>, Fawang Ye<sup>1,\*</sup>, Chuan Zhang<sup>1</sup> and Zhaodong Xi<sup>2</sup> 

<sup>1</sup> National Key Lab of Remote Sensing Information and Imagery Analysis, Beijing Research Institute of Uranium Geology, Beijing 100029, China

<sup>2</sup> School of Energy Resource, China University of Geosciences (Beijing), Beijing 100083, China

\* Correspondence: yfwbeijing2008@sina.com

**Abstract:** The Carboniferous–Permian, coal-bearing, sedimentary succession on the eastern edge of the Ordos Basin in the Shilouan Block contains large accumulations of hydrocarbon resources. During the exploration of coalbed methane and tight sandstone gas in the study area, multiple drilling wells in the tight sandstone reservoirs have yielded favorable gas logging results. The Benxi, Taiyuan, Shanxi, Shihezi, and Shiqianfeng formations contain multiple sets of sandstone reservoirs, and the reservoir quality and the controlling factors of its tight sandstones were affected by sedimentation, diagenetic alteration, and pore structure. This study comprehensively examines the sedimentary environment, distribution of sand bodies, and physical characteristics of tight sandstone reservoirs through drilling, coring, logging, and experimental testing. The results indicate that the Carboniferous–Permian tight sandstones are mainly composed of lithic sandstone and lithic quartz sandstone. The reservoir quality is relatively poor, with an average permeability of 0.705 mD and porosity of 6.20%. The development of reservoirs in the study area is primarily influenced by diagenesis and sedimentation. Compaction and cementation, which are destructive diagenetic processes, significantly reduced the porosity of the sandstone reservoirs in the study area. Compaction primarily causes a reduction in porosity and accounts for over 70% of the overall decrease in porosity. Dissolution, as a constructive diagenetic process, has a limited effect on porosity and is the primary reason for the relatively tight nature of these reservoirs. The macroscopic and microscopic characteristics of tight sandstone reservoirs were used to establish the evaluation and classification criteria, after which the sandstone reservoirs in the study area were divided into three types. The poor quality type II and type III reservoirs are predominant, while high quality type I reservoirs are primarily limited to the Shihezi Formation.

**Keywords:** tight sandstone gas; reservoir; pore structure; diagenesis; porosity



**Citation:** Wang, J.; Ye, F.; Zhang, C.; Xi, Z. Factors That Control the Reservoir Quality of the Carboniferous–Permian Tight Sandstones in the Shilouan Block, Ordos Basin. *Processes* **2023**, *11*, 2279. <https://doi.org/10.3390/pr11082279>

Academic Editor: Carlos Sierra Fernández

Received: 25 June 2023

Revised: 25 July 2023

Accepted: 26 July 2023

Published: 28 July 2023



**Copyright:** © 2023 by the authors. Licensee MDPI, Basel, Switzerland. This article is an open access article distributed under the terms and conditions of the Creative Commons Attribution (CC BY) license (<https://creativecommons.org/licenses/by/4.0/>).

## 1. Introduction

Tight sandstone gas is an important unconventional natural gas. Tight gas reservoirs typically have an effective permeability of less than 0.1 mD (or an absolute permeability of less than 1 mD) and a porosity of less than 10% [1–3]. A diverse array of tight sandstone gas reservoirs with significant economic potential occurs across China. Progress in unconventional oil and gas exploration technologies has allowed for the identification of basins such as the Ordos, the Tarim, and the Songliao, where geological conditions are also conducive to the formation of tight sandstone gas reservoirs [4]. The annual production of tight sandstone gas in the Ordos Basin surpassed  $3 \times 10^{10}$  m<sup>3</sup> in 2010, with proven reserves exceeding  $2 \times 10^8$  m<sup>3</sup>. Tight sandstone gas accounts for over one third of China's natural gas energy structure, making China one of the leading global producers of tight sandstone gas after the United States and Canada [4,5].

Tight sandstone gas reservoirs are extensively distributed in the Upper Paleozoic strata of the Ordos Basin and occur primarily within the Carboniferous–Permian Taiyuan, Shanxi, and Shihezi formations, where these formations serve as the principal layers for tight sandstone gas production. Despite the widespread occurrence of sandstone across the Ordos Basin, its compositional and structural maturity is relatively low. Under surface conditions, a significant portion of the samples have porosity levels below 10%, and approximately 90% of the reservoirs have a matrix permeability below 0.1 mD under overburdened pressure conditions [6,7]. The development of tight sandstone reservoirs is primarily influenced by sedimentation, diagenesis, and tectonism. Sedimentation plays the largest role in the formation of low-permeability reservoirs and determines the types of diagenesis that occur. Diagenesis is the key driver in creating ultra-low porosity and permeability reservoirs, while tectonic processes transform tight sandstone reservoirs [8–11]. Advances in research methods and technologies have allowed for substantial progress in studying the characteristics and controlling factors in the development of tight sandstone reservoirs. Advanced technologies that have been used in reservoir characterization include high-precision and high-resolution microscopic observation, fluid inclusion testing, mineralogical composition identification, genetic analysis, and pore system characterization [12–14]. These technologies and research methods provide a reliable foundation for analyzing pore genesis, diagenesis types, and diagenetic evolution, and shift the study of tight sandstone reservoir characteristics and their controlling factors from a qualitative description to a quantitative study.

The tight sandstone formation associated with the Carboniferous–Permian coal measure in the eastern margin of the Ordos Basin exhibits a stable horizontal thickness distribution and vertical multi-layer superposition. This formation offers promising prospects for the exploration and development of tight sandstone gas. This study used experimental methods, such as thin section petrographic examinations, mercury intrusion, and porosity and permeability testing, to determine the distribution and reservoir characteristics of the sandstone formation of the Shilouan Block. The influence of sedimentation, diagenesis, and pore structure on the physical properties of tight sandstone reservoirs has also been investigated and provides valuable guidance for the exploration and development of tight sandstone gas in the Shilouan Block.

## 2. Geological Setting

### 2.1. Structural Characteristics and Stratigraphy

The Shilouan Block is situated in the southern part of the Jinxi Flexural Belt within the Ordos Basin. It shows an overall structural pattern known as “two uplifts and two depressions”. The “two uplifts” are the Shilou Anticline and the Xixian Anticline, with the eastern wing of the Shilou Anticline being intersected by a nearly north–south westward dipping thrust fault. This fault causes a steeper eastern wing when compared to the western wing. The “two depressions” consist of the Caocun Fold Belt and the Xixiandong Syncline. The structural characteristics of the study area primarily involve north–south and northeast folding and flexing, accompanied by a significant presence of faults in the region (Figure 1).

The Upper Paleozoic strata in the Shilouan Block are well developed, with the lowermost part of the sedimentary succession consisting of Middle Ordovician limestones of the Majiagou Formation. The Middle Carboniferous Benxi Formations, which are characterized by a parallel unconformity, overlay the Ordovician limestones. The coal-bearing strata within this block include the Middle Carboniferous Benxi Formation, the Upper Carboniferous Taiyuan Formation, and the Lower Permian Shanxi Formation. Additionally, the uppermost part of the sedimentary succession is represented by the Shihezi Formation and the Shiqianfeng Formation (Figure 2).

### 2.2. Sedimentary Facies and Sand Body Distribution

The Shilouan Block is extensively developed in the Upper Paleozoic sandstones. It consists primarily of the tidal flat sandstones from the Taiyuan Formation and the channel

sandstones from the Shanxi, Shihezi, and Shiqianfeng formations, as well as beach bar sandstones. A depositional hiatus occurred during the Middle Ordovician and the Early Carboniferous. During the sedimentation period of the Benxi Formation in the Middle Carboniferous, the Ordos Basin gradually underwent subsidence as seawater infiltrated from the east and southeast. The sediments from the Shilounan Block in the Ordos basin were deposited in an epicontinental sea. The sedimentary characteristics of the Taiyuan Formation are similar to the Benxi period, where the Shilounan Block received sediment from areas northeast and northwest of the Ordos basin. This caused the development of tidal flats, barrier islands, and lagoon deposits (Figure 3a). The sand bodies in this formation consist of gray fine-grained sandstones and light gray siltstones, and have a maximum sedimentary thickness of 14.8 m. The Shanxi Formation was predominantly deposited in the delta plain subfacies and is characterized by distributary channel sands that form the main sand body (Figure 3b). The sand body exhibits a northwest–southeast distribution trend and ranges in thickness from 5 to 30 m.

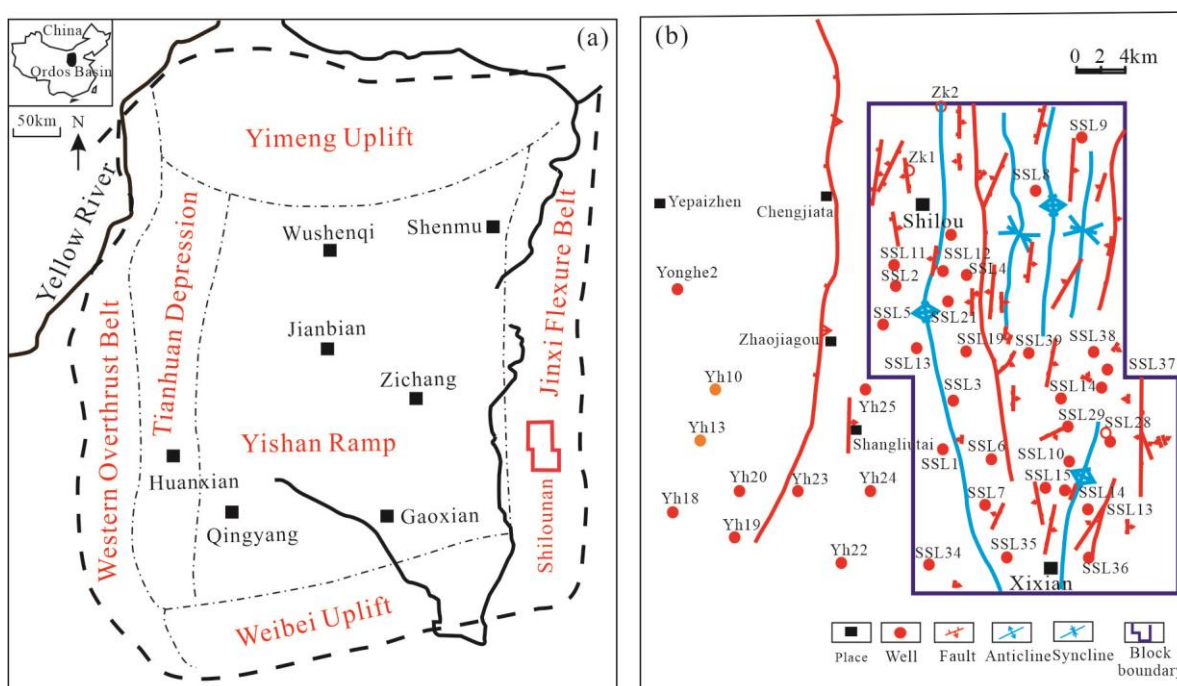


**Figure 1.** (a) The tectonic divisions of the Ordos Basin and the location of the Shilounan Block (irregular polygon colored in red); (b) structural map of the Shilounan Block.

The climate transitioned from warm and humid to arid and hot during the sedimentation of the Xiashihezi Formation, which significantly reduced the vegetation. A series of gray-white to yellow-green terrigenous debris, which developed the delta front subfacies, was deposited during this period. The main sedimentary microfacies comprised underwater distributary channels and underwater interdistributary bays, with the presence of underwater distributary channel sand bodies (Figure 3c). The sediments of the Shangshihezi Formation are characterized by purplish-red and yellowish-green hues. These colors indicate a lithofacies paleogeographic environment where delta and shallow lake conditions coexisted. Within the Shilounan Block, the delta front subfacies are characterized by the presence of underwater distributary channel sand bodies (Figure 3d). A series of purplish-red clastic rocks were deposited during the sedimentation of the Shiqianfeng Formation. This area mainly exhibits the development of delta front subfacies and shore-shallow lake facies, with the presence of underwater distributary channel sand bodies (Figure 3e).

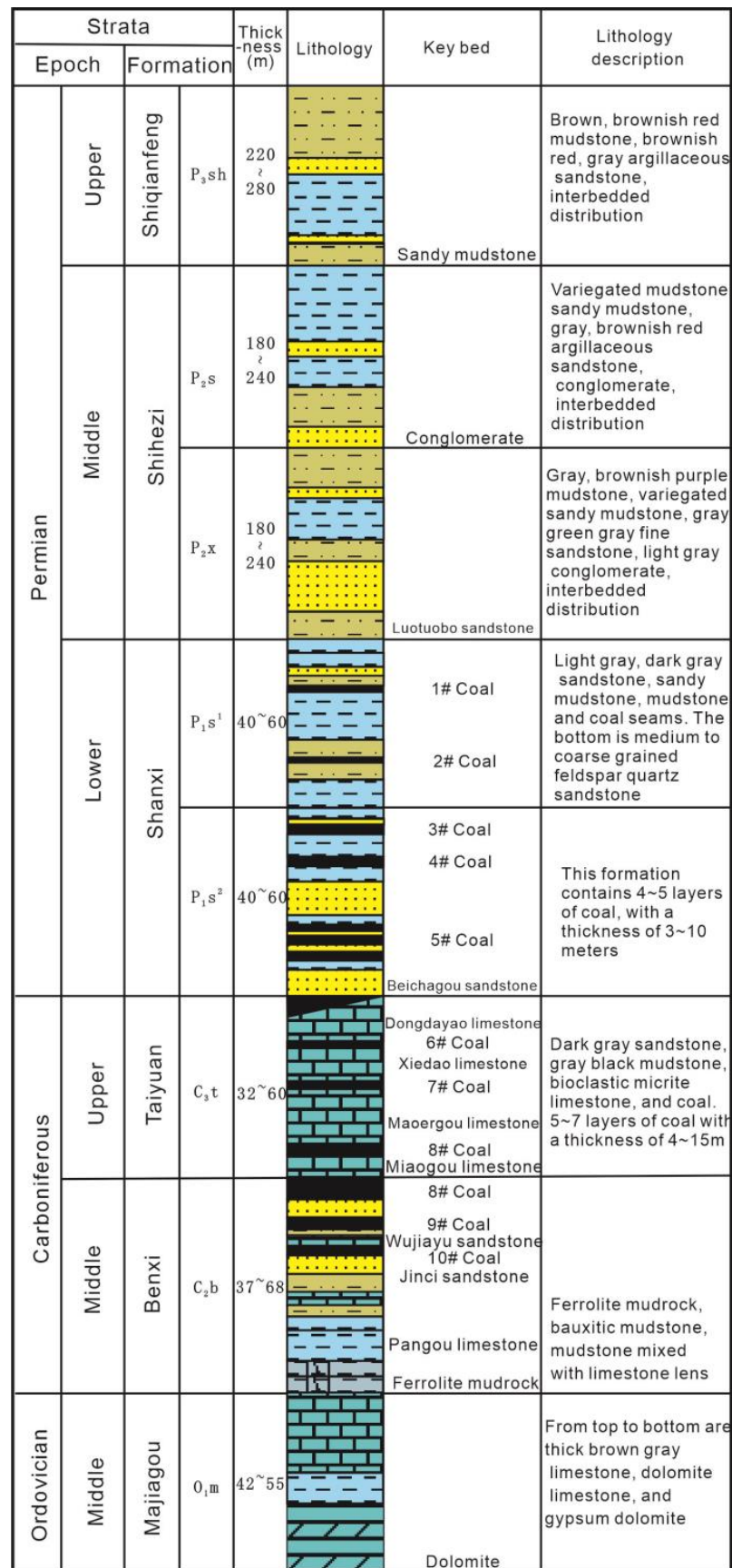
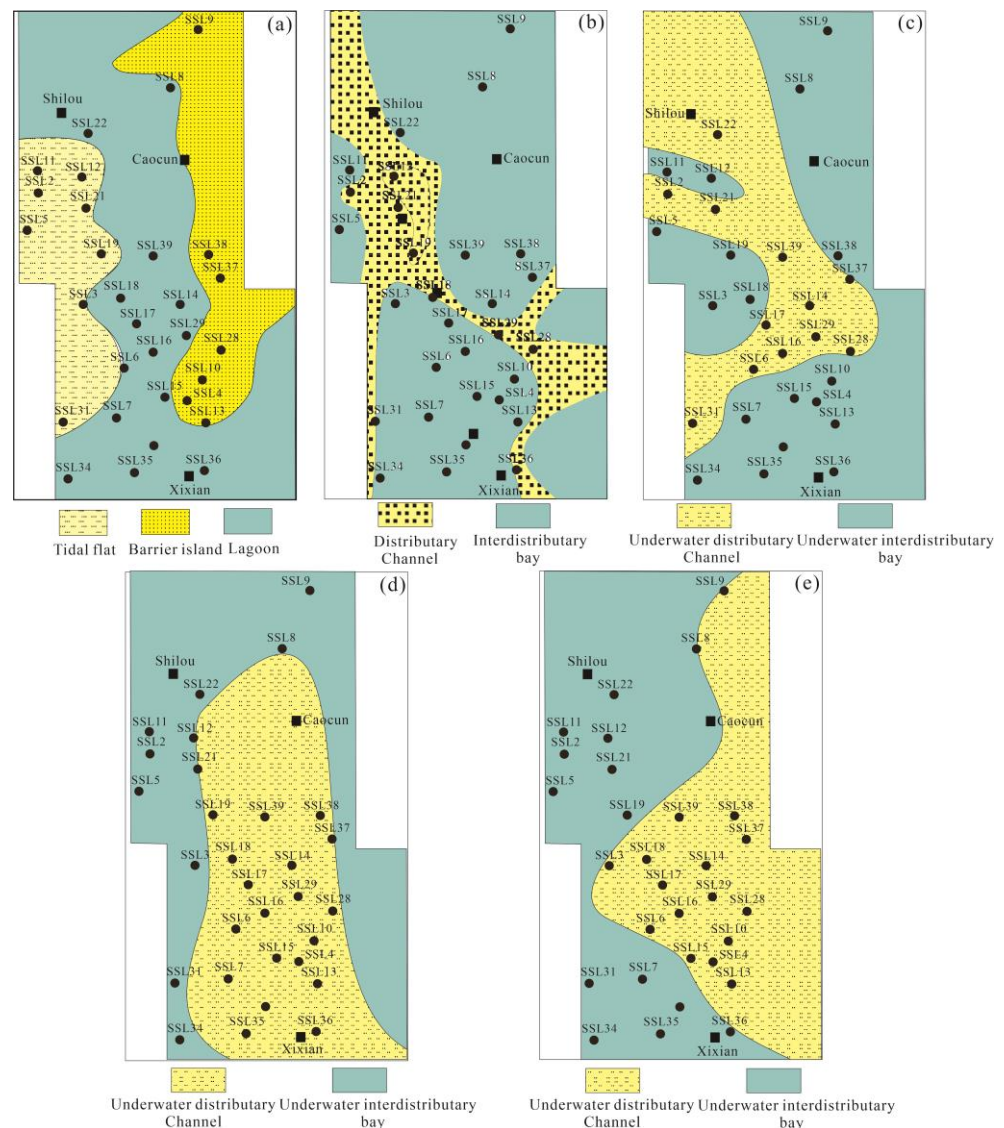


Figure 2. Comprehensive lithostratigraphic column of the Shilouan Block.



**Figure 3.** Distribution of the sedimentary facies and sand bodies within the study area (the Shilounan Block): (a) Taiyuan Formation, (b) Shanxi Formation, (c) Xiashihezi Formation, (d) Shangshihezi Formation, (e) Shiqianfeng Formation. Dots represent well locations and rectangles represent cities.

### 3. Sampling and Methodology

More than 280 samples were collected from 28 drilling wells in the Shilounan Block, with the main sampling layers including the Benxi, Taiyuan, Shanxi, Shihezi, and Shiqianfeng formations. Figure 1b shows the distribution of the well locations for sampling. The samples were analyzed via thin section petrographic examinations, SEM, porosity and permeability measurements, XRD analysis, and mercury intrusion tests. The specific details of the experimental methods and detailed procedures are based on previous papers published by our team [15,16].

## 4. Results

### 4.1. Petrological Characteristics

The sandstones from the Taiyuan and Shanxi formations range primarily from dark gray to gray. In contrast, the sandstones from the Shihezi Formation range from gray to gray-white to gray-green. The sandstones of the Shiqianfeng Formation, however, showcase a more diverse range of colors that range from mainly brown to grayish-green and purple-red. There is a notable color variation in the sandstones from the Benxi Formation and the

Shiqianfeng Formation, where the formations transition from gray and black to green and grayish-brown. These color changes indicate a shift from reducing to oxidizing conditions and a transition in climate from humid to arid in the sedimentary environment during the late Paleozoic (Figure 4).

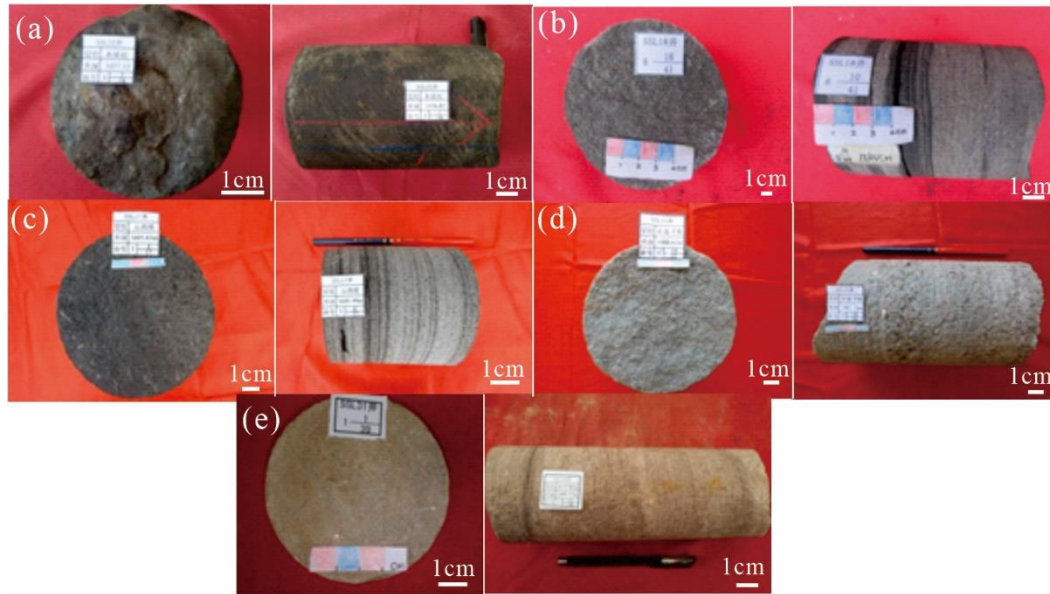


**Figure 4.** Core characteristics of the Carboniferous–Permian sandstones in the study area: (a) dark gray siltstone of the Benxi Formation; (b) gray medium-grained sandstone of the Taiyuan Formation; (c) gray fine-grained sandstone with carbonaceous and argillaceous material and muscovite fragments of the Shanxi Formation; (d) gray-green sandstone of the Shihezi Formation; (e) grayish brown fine-grained sandstone of the Shiqianfeng Formation.

The Shilounan Block contains several types of sandstones, such as lithic sandstone, lithic feldspathic sandstone, lithic quartz sandstone, quartz sandstone, and feldspathic lithic sandstone (Figure 5). Within the Taiyuan and Shanxi formations, three main types of sandstone are present—lithic sandstone, lithic quartz sandstone, and quartz sandstone. The quartz content varies from 10% to 96%, with an average quartz content of 53.2%. The rock debris content ranges from 1% to 70%, with an average rock debris content of 28.9%. The feldspar content in the Taiyuan and Shanxi formations is relatively low and is present as fine to medium feldspar grains.

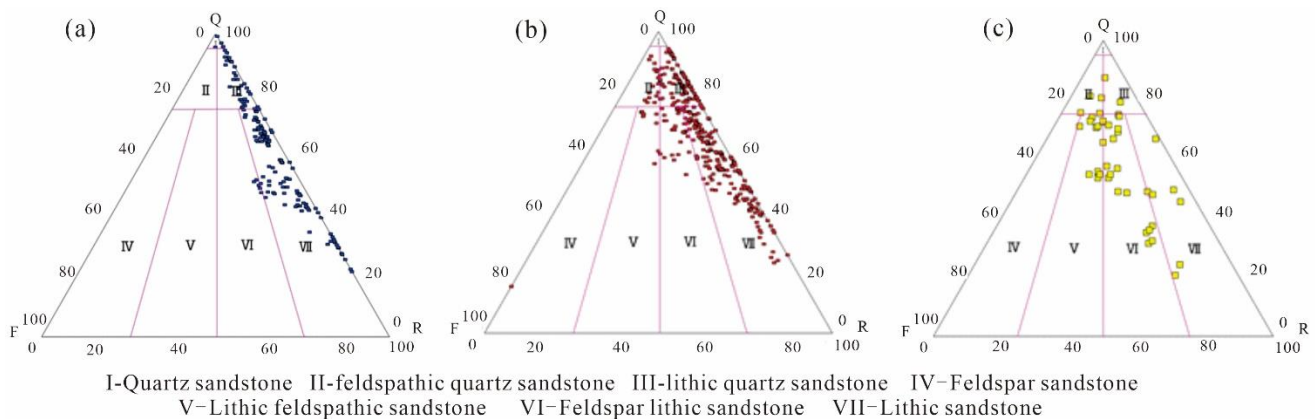


**Figure 5.** Sandstone types identified in the Carboniferous–Permian sediments from the Shilounan Block study area: (a) Taiyuan and Shanxi formations, (b) Shihezi Formation, (c) Shiqianfeng Formation. Q = quartz; F = feldspar; R = rock fragments.

The Shihezi Formation primarily comprises lithic sandstone, commonly known as lithic quartz sandstone, feldspathic lithic sandstone, and quartz sandstone. The quartz content within this formation ranges from 14% to 89%, while the rock debris content ranges from 2% to 63%, with an average content of 26.1%. In contrast, the sandstones of the Shiqianfeng Formation are predominantly composed of lithic feldspathic sandstone and feldspathic lithic sandstone, and are occasionally accompanied by lithic sandstone and feldspathic quartz sandstone. The feldspar content in the Shihezi Formation is relatively high. Quartz is the predominant mineral in the sandstone, with the highest content being observed in the Taiyuan Formation and the lowest content being observed in the Shiqianfeng Formation.

#### 4.2. Porosity and Permeability

Porosity and permeability tests were conducted on 245 sandstone samples from the Shilouan Block. The samples have an average porosity of 6.2% and an average permeability of only 0.705 mD. The reservoir, therefore, has low porosity and ultra-low permeability (Table 1).

**Table 1.** Porosity and permeability of the sandstones from the study area.

Formation	Shangshihezi	Xiashihezi	Shanxi	Taiyuan	Benxi
Porosity /%	8.4 (101)	7.1 (94)	3.99 (11)	6.88 (2)	4.9 (4)
Permeability /mD	0.95 (97)	0.29 (93)	0.11 (11)	0.77 (2)	2.86 (4)

Note: The numbers in the parentheses indicate the number of samples.

The Shihezi Formation has the highest porosity, with an average of 7.7%. The Shangshihezi Formation has an average porosity of 8.4%, while the Xiashihezi Formation has an average porosity of 7.1%. The sandstones in the Xiashihezi Formation display a maximum porosity of 15.4% and a minimum porosity of 1.3%. Porosities that exceed 10% account for only 10% of the samples (Figure 6a). The sandstone in the Shangshihezi Formation ranges from a maximum porosity of 16.1% to a minimum porosity of 1.6%. Here, approximately 50% of the samples exhibit porosity exceeding 10%, indicating favorable reservoir characteristics (Table 1 and Figure 6a). Even though the Taiyuan Formation has a porosity close to 7%, the sample size is relatively small and shows higher variability. The Shanxi and Benxi formations have average porosities of 4.0% and 4.9%, respectively.

The limited number of samples from the Benxi and Taiyuan formations exhibit relatively high permeabilities. The average permeability is 0.11 mD in the Shanxi Formation, 0.29 mD in the Xiashihezi Formation, and 0.95 mD in the Shangshihezi Formation. The permeability range of the Shihezi Formation is quite extensive, with the Xiashihezi Formation displaying a maximum permeability of 6.14 mD and a minimum of only 0.0013 mD (Figure 6b). Similarly, the Shangshihezi Formation has a maximum permeability of 14.18 mD and a minimum of 0.0033 mD. The peak permeability of the Xiashihezi Formation ranges from 0.1 to 0.5 mD, while the peak permeability of the Shangshihezi Formation ranges from 0.1 to 0.5 mD and exceeds 2 mD (Figure 6b).

Even though the data points on the porosity and permeability of the sandstone reservoirs in the study area are relatively scattered, they exhibit a certain degree of correlation (Figure 7). This correlation suggests that the physical properties are influenced by multiple factors rather than a single geological factor. The variations in the sedimentary background, the burial depth, the lithology of the roof and floor, and the heterogeneity of diagenesis, all contribute to the weak correlation between the porosity and the permeability [17,18]. Cai (2015) also observed a similar weak positive correlation between the porosity and the permeability when investigating the Chang 8 reservoir in the Jiyuan area of the Ordos Basin [19].

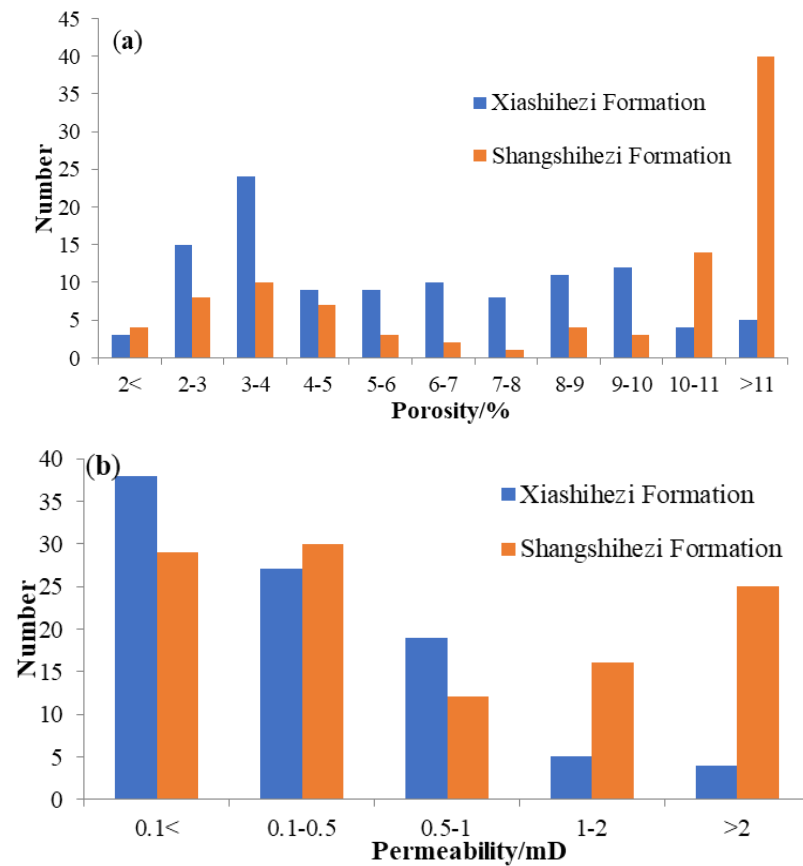


**Figure 6.** Distribution of porosity and permeability in the sandstone reservoirs from the Shihezi Formation in the study area: (a) Distribution of porosity, and (b) Distribution of permeability.

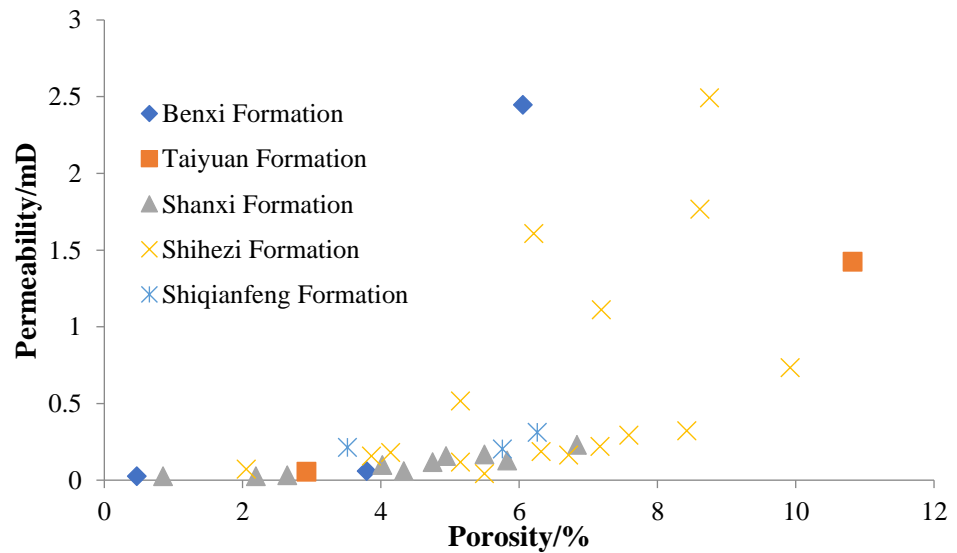


**Figure 7.** Relationship between porosity and permeability in Carboniferous–Permian sandstone samples.

### 4.3. Pore System

#### 4.3.1. Pore Type

Petrographical examinations and statistical analysis of 117 sandstone cast thin sections, combined with scanning electron microscopy (SEM) analysis, were used to classify the pore types into residual intergranular pores, dissolution pores, and intercrystalline pores.

Residual intergranular pores: the primary intergranular pores are almost imperceptible, while the residual intergranular pores are predominantly observed. The residual intergranular pores are mainly formed due to compaction and cementation, and exhibit triangular or polygonal shapes with fairly straight pore boundaries. There is limited connectivity and significant heterogeneity among these isolated pores because the distribution of the residual intergranular pores is primarily isolated (Figure 8).

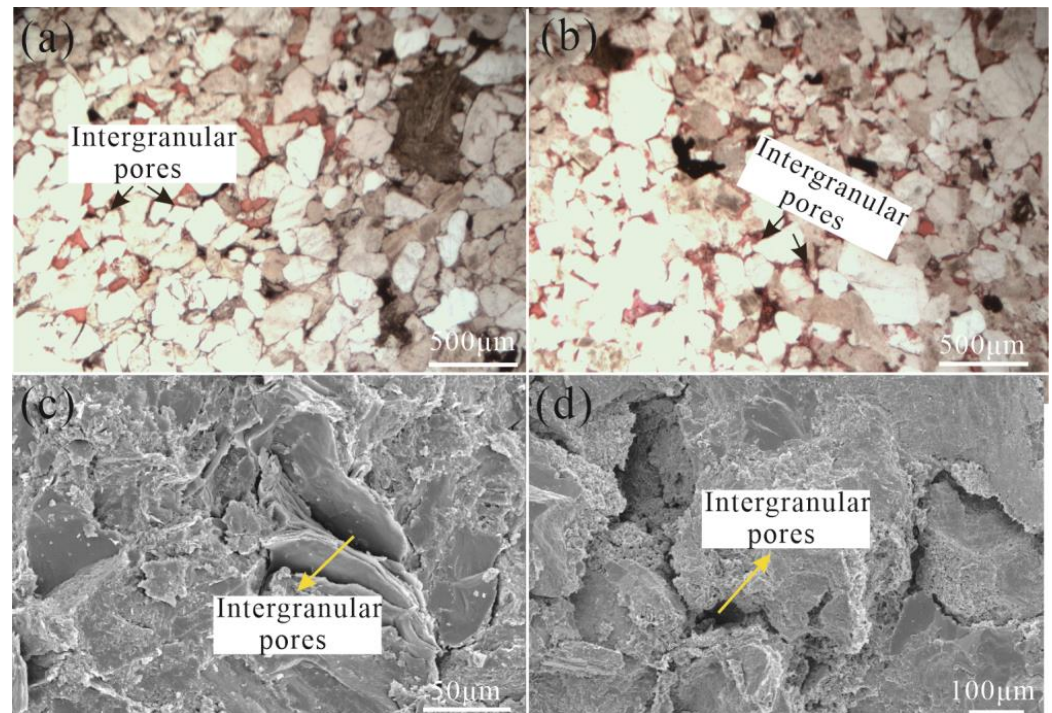


**Figure 8.** Microscopic images of polished thin sections and high-resolution SEM images of residual intergranular pores: (a) medium-grained feldspathic sandstone, with small residual intergranular pores; (b) medium-grained feldspathic sandstone, with small residual intergranular pores; (c) particles that are bent due to compaction, causing the irregular morphology of the intergranular pores; (d) kaolinite aggregates and illite crystals between particles, with development of residual intergranular pores within these aggregates.

Dissolved pores: the dissolved pores consist of intergranular pores and intragranular pores (Figure 9a–d). The feldspar, rock debris, and clay minerals are susceptible to dissolution. The intergranular pores are large due to the partial or complete erosion of larger minerals such as feldspars. The intergranular pores tend to have good connectivity and an irregular morphology, and feature multilateral and harbor-shaped structures. The intragranular pores, in contrast, are predominantly circular and elliptical, with relatively limited connectivity. These pores are mainly present within the rock debris particles.

Intercrystalline pores: the clay minerals kaolinite and illite are commonly found in this rock. Kaolinite typically forms through feldspar alteration and often exhibits a book-like or plate-like structure. Illite is predominantly fibrous and filamentous, with numerous pores developed within its aggregates (Figure 9e,f).

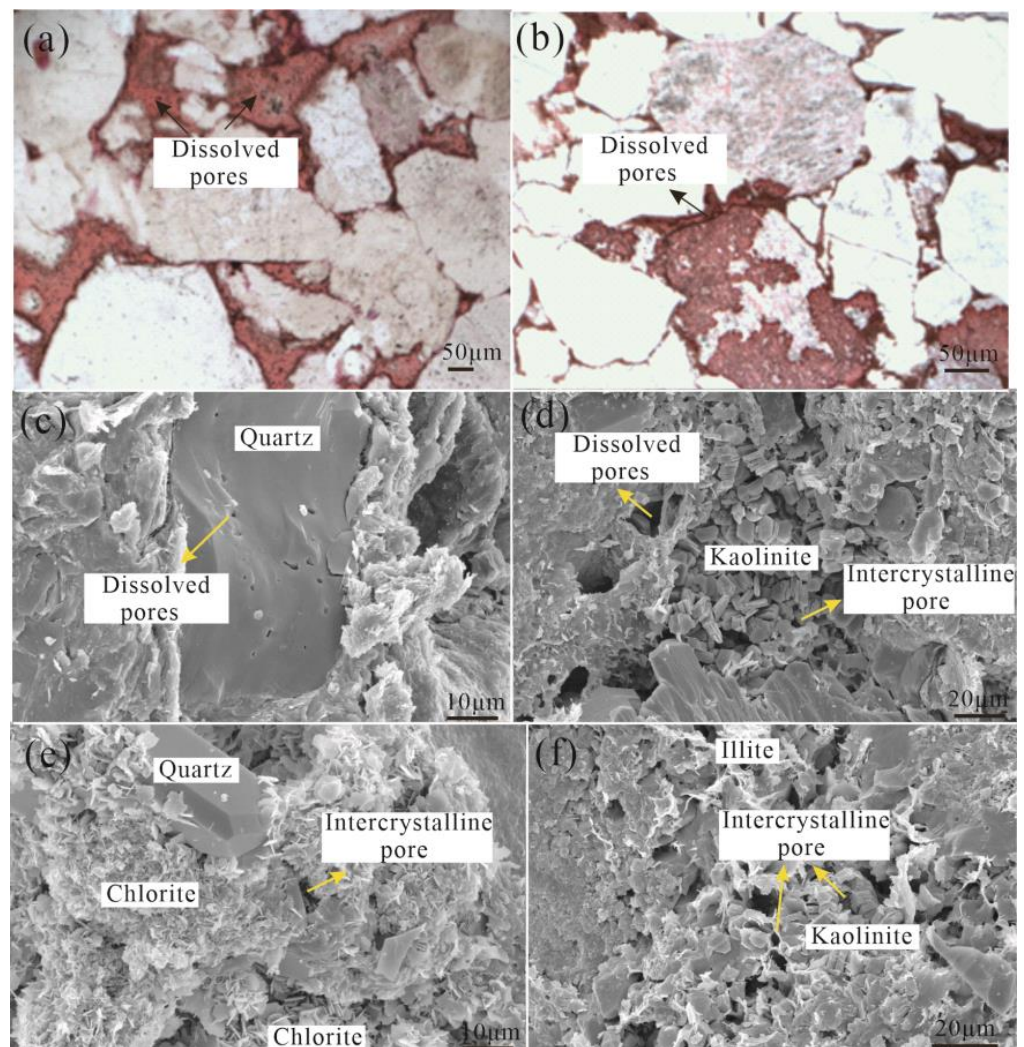


**Figure 9.** Microscopic images of polished thin sections and high-resolution SEM images of the dissolved pores and intercrystalline pores: (a) fine- to medium-grained feldspathic sandstone, with well-developed pores that formed due to feldspar dissolution; (b) coarse-grained lithic quartz sandstone exhibiting significant feldspar that was corroded to form well-developed dissolved pores; (c) illite-wrapped quartz particle surfaces with limited dissolved pores; (d) intergranular pores filled with kaolinite aggregates, along with developed intercrystalline micropores and dissolved pores; (e) chlorite aggregate covering particle surfaces, intermixed with authigenic quartz crystals, and displaying developed intergranular micropores; (f) intergranular pores filled with kaolinite and illite aggregates, accompanied by developed intercrystalline micropores.

#### 4.3.2. Pore Structure

The pore structure of the sandstone in the Shilouan Block is categorized into three types based on the pore structure parameters and the capillary pressure curve derived from the mercury intrusion measurements of the 29 sandstone samples, the observations of the cast thin sections, and the SEM (Table 2 and Figure 10).

**Table 2.** Pore structure parameters and classification of pore structure types based on mercury intrusion testing.

Pore Type	Sample ID	Formation	Sorting Coefficient	Structural Coefficient	Coefficient of Mean Value	Average Pore Throat Diameter/ $\mu\text{m}$	Displacement Pressure/MPa	Maximum Mercury Saturation/%	Efficiency of Mercury Ejection/%	Porosity /%
I	S6-5	Xiashi hezi	2.89	3.25	0.16	0.97	0.23	69.03	37.59	3.1
	S6-18	Xiashi hezi	0.87	2.3	0.46	0.37	0.99	81.08	43.38	8.2
	S6-19	Xiashi hezi	1.12	3.42	0.22	0.44	0.79	80.09	38.76	7.2
	S7-6	Xiashi hezi	1.52	1.59	0.3	0.59	0.61	86.85	51.68	12.4
	S7-7	Xiashi hezi	1.62	1.67	0.32	0.62	0.59	84.59	42.85	10.8
	S1-2	Xiashi hezi	0.23	0.08	/	2.48	0.7	84.6	39.8	7.7
	S1-3	Xiashi hezi	0.2	0.17	/	0.31	0.7	91.54	35.92	7
	S1-4	Xiashi hezi	0.21	0.15	/	0.31	0.5	88	42.02	8.6
	S2-22	Shang shihezi	0.21	0.13	/	0.33	0.3	86.89	46.63	16.8
	S2-38	Shang shihezi	0.28	0.19	/	0.41	0.3	79.63	45.26	10.6
	S2-47	Shang shihezi	0.26	0.03	/	0.48	0.3	84.33	35.91	13.8
		Average		0.86	1.18	0.29	0.66	0.55	83.33	41.8
II	S12-44	Tai yuan	11.2	9.58	0.35	3.66	0.12	85.4	20.08	7.9
	S12-45	Tai yuan	13.2	14.5	0.32	4.26	0.11	75.89	16.19	8.4
	S2-17	Shang shihezi	0.12	0.01	/	0.02	7	90.65	22.28	4
	S2-30	Shang shihezi	0.2	0.2	/	0.38	0.5	86.69	30.17	12.2
	S6-2	Shanxi	0.63	1.06	0.33	0.28	1.65	81.67	26.28	3.6

Table 2. Cont.

Pore Type	Sample ID	Formation	Sorting Coefficient	Structural Coefficient	Coefficient of Mean Value	Average Pore Throat Diameter/ $\mu\text{m}$	Displacement Pressure/MPa	Maximum Mercury Saturation/%	Efficiency of Mercury Ejection/%	Porosity /%
II	S12-13	Shang shihezi	2.2	5.09	0.24	0.77	0.38	76.89	33.41	9.9
	S12-14	Shang shihezi	5.2	40.8	0.23	1.64	0.19	61.57	21.18	12.6
	S1-1	Xiashi hezi	0.48	0.05	/	0.11	1	63.57	33.38	2.5
	S2-9	Shanxi	0.52	0.1	/	0.17	0.8	62.45	31.29	4
	S2-14	Shanxi	0.69	0.01	/	0.02	7	51.08	31.73	3.2
	Average			3.43	7.14	0.29	1.13	1.87	73.58	26.6
III	S6-3	Tai yuan	0.52	1.04	0.39	0.27	1.12	37.42	32.92	3.2
	S6-4	Tai yuan	1.92	0.87	0.24	0.72	0.45	38.98	36.1	5.6
	S6-9	Tai yuan	0.04	0.08	0.6	6.88	6.88	30.79	35.6	2.7
	S2-2	Tai yuan	1.05	0.13	/	0.14	1.5	37.4	44.52	5.2
	S2-52	Xiashi hezi	0.55	0.05	/	0.09	2	59.42	38.08	4
	S2-62	Xiashi hezi	1.66	0.03	/	0.06	3	22.3	33.61	5.7
	S2-67	Xiashi hezi	1.06	0.04	/	0.05	3	36.75	36.2	3.7
	S2-75	Xiashi hezi	1.05	0.13	/	0.14	1.5	37.4	44.52	5.2
Average			0.98	0.3	0.41	1.04	2.43	37.56	37.69	4.4

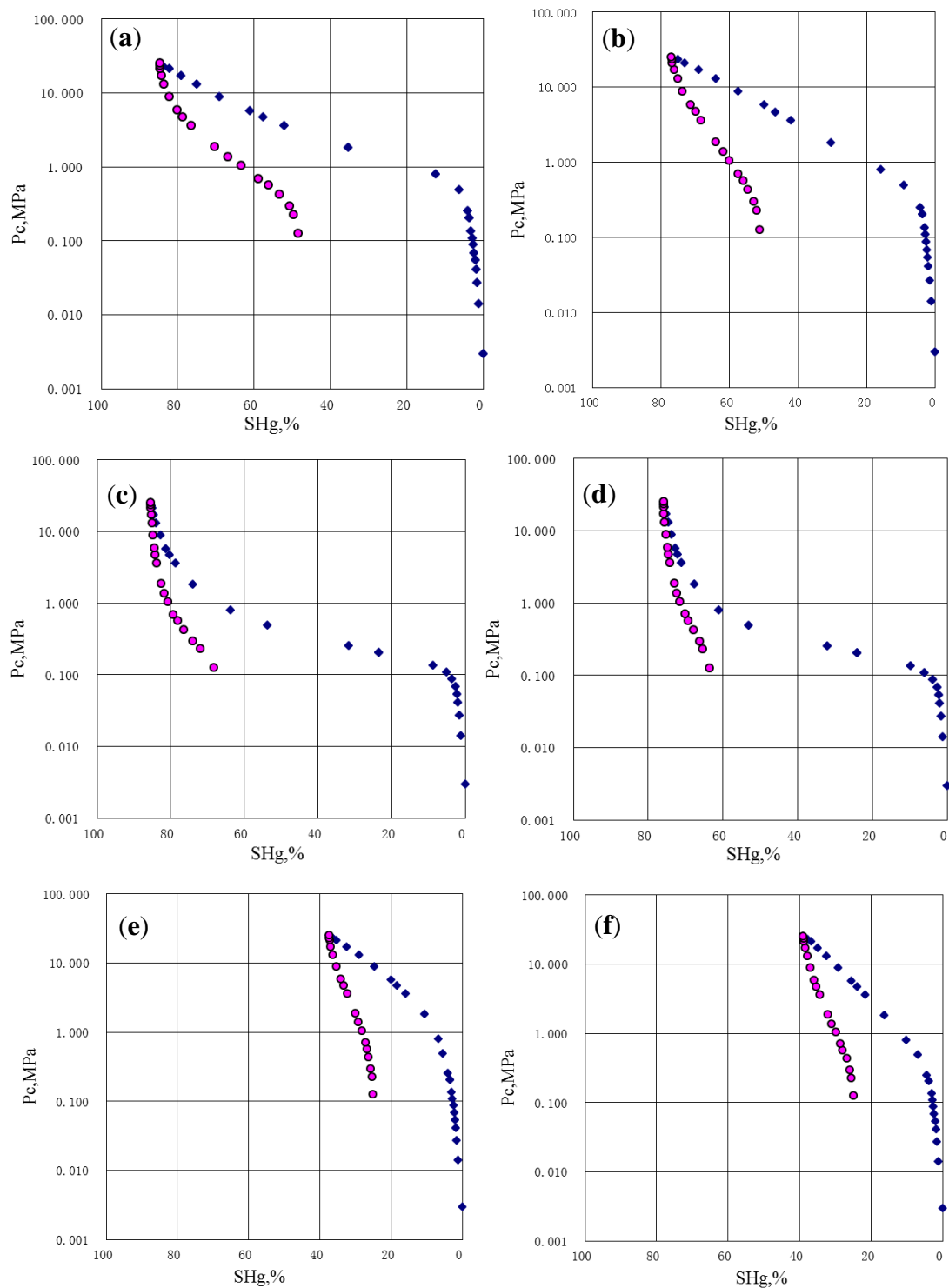


**Figure 10.** Mercury intrusion curves of three types of sandstone samples in the study area. Porosity type I: (a,b); type II: (c,d); type III: (e,f). The blue circles indicate inject mercury quantity curve, and the red circles indicate withdrawal mercury quantity curve.

Type I: the displacement pressure of a reservoir with the type 1 pore structure ranges from 0.3 to 0.99 MPa, with an average of 0.55 MPa. The average pore throat size ranges from 0.31 to 2.48  $\mu\text{m}$ , indicating relatively small pore throats, while the sorting coefficient is relatively low. The average maximum mercury saturation reached 85%, with over 40% of the mercury being efficiently ejected (with an average mercury injection porosity of 9.65%). The capillary pressure curve has a gentle slope, deviating towards the bottom left of the graph.

It was initially only possible to inject a small amount of mercury, suggesting the absence of well-developed fractures and large pores. However, at 0.1 MPa pressure, a significant amount of mercury entered the pores, indicating good pore connectivity. The pore morphology is predominantly cylindrical and parallel plate-shaped (Figure 10a,b). Sandstone reservoirs with such pore structures generally exhibit favorable physical properties.

Type II: the displacement pressure of a reservoir with the type II pore structure is relatively high, ranging from 0.11 to 7 MPa, with an average of 1.87 MPa. The average pore throat size ranges from 0.02 to 4.26  $\mu\text{m}$ . The sorting coefficient of the type II pore structure is relatively high, and the average maximum mercury saturation reaches 73%. However, the efficiency of mercury ejection is low at only 26.6%, yielding an average mercury injection porosity of 6.83%. The volume of mercury increases slowly when the pressure reaches 0.1 MPa, but rapidly increases when the pressure reaches 1 MPa (Figure 10c,d). These results indicate the presence of relatively well-developed small-sized pores within which a significant amount of mercury gets trapped. Sandstone reservoirs with the type II pore structure have a relatively high porosity but poor connectivity.

Type III: the mercury intrusion curve of a reservoir with the type III pore structure exhibits a steep slope and upward convexity, leaning towards the upper right part of the figure (Figure 10e,f). Both the mercury saturation and efficiency of mercury ejection are below 40%, indicating limited available pore space for mercury intrusion. The average porosity of this type of reservoir is 4.4%, suggesting poor suitability for gas storage and gas seepage.

The Shihezi Formation mainly has sandstone reservoirs with type I and type II pore structures. These reservoirs exhibit fairly well-developed dissolution pores and residual intergranular pores, resulting in higher porosity and better connectivity. These pore structures are primarily formed in a delta front environment. Sandstone reservoirs with a type III pore structure, however, have low porosity and limited connectivity. The Taiyuan Formation consists of many of these reservoirs.

## 5. Discussion

### 5.1. Sedimentation Controls on Reservoir Quality

Sedimentary facies play a crucial role in controlling the development and distribution characteristics of sandstone reservoirs. The Taiyuan Formation is primarily composed of tidal flat and lagoon deposits, while the Shanxi Formation consists predominantly of delta plain deposits. The Shihezi Formation is characterized by delta front deposits, while the Shiqianfeng Formation is dominated by shore shallow lake and delta facies. The physical parameters of the sandstone reservoirs vary across the different sedimentary facies zones (Table 3). The sandstone reservoirs in the Shihezi Formation exhibit favorable reservoir properties, such as high porosity and good connectivity. The barrier sandstone reservoirs in the Taiyuan Formation and the distributary channel sandstone reservoirs in the Shanxi Formation, however, exhibit low porosity and permeability. The low porosity and permeability are due to the frequent marine invasion and regression events during their sedimentation period that have led to the interbedding of sand and mudstone [20]. The pore structures have become complex, while the pore tortuosity increased. It is important to note that even sandstone reservoirs that formed in the same sedimentary facies can exhibit significant differences in their properties [21,22]. Sandstone reservoirs that developed in the central areas of river channels, such as those in the Shihezi Formation, generally have better porosity and permeability compared to those developed in the inter-channel or two-wing regions of the river channel.

**Table 3.** Porosity and permeability of sandstone reservoirs in different sedimentary facies in the study area.

Formation	Sedimentary Facies	Porosity (%)		Permeability (mD)	
		Range	Average	Range	Average
Shangshihezi	Delta Front	0.51–15.34	8.4	0.06–2.31	0.95
Xiashihezi	Delta Front	0.23–14.34	7.1	0.04–0.79	0.29
Shanxi	Distributary Channel	1.43–5.89	3.99	0.007–0.45	0.11
Taiyuan	Tidal Flat Lagoon	4.56–9.2	6.88	0.002–3.64	0.77

Sandstones that formed under different sedimentary conditions can exhibit significant variations in their mineral composition, thickness, distribution, particle size, sorting, and rounding. These further increase the substantial differences in the reservoir properties [23,24]. A positive correlation is observed between quartz content and porosity, indicating that porosity tends to increase with higher quartz content (Figure 11a). The sediments in the study area have experienced deep burial (>1500 m) and significant compaction and pressure dissolution. Since quartz is a rigid mineral, it enhances the rock's ability to withstand compression and preserves some primary intergranular pores [25,26]. Quartz also serves as the material basis for the formation of secondary dissolution pores, and there is a positive correlation between the porosity and the quartz content of the sediment. There is, however, a negative correlation between rock fragments and porosity since higher rock fragment content decreases the porosity (Figure 11c). Unlike quartz, rock fragments have smaller particle sizes which can easily block pores. Sandstone-type reservoirs with higher quartz content (for example quartz sandstone) usually have higher porosities compared to samples with a higher rock fragment content, such as lithic sandstone. No significant correlation was observed between the content of quartz and rock fragments and the permeability (Figure 11b,d). This means that quartz and rock fragments are not the primary controlling factors that influence permeability.

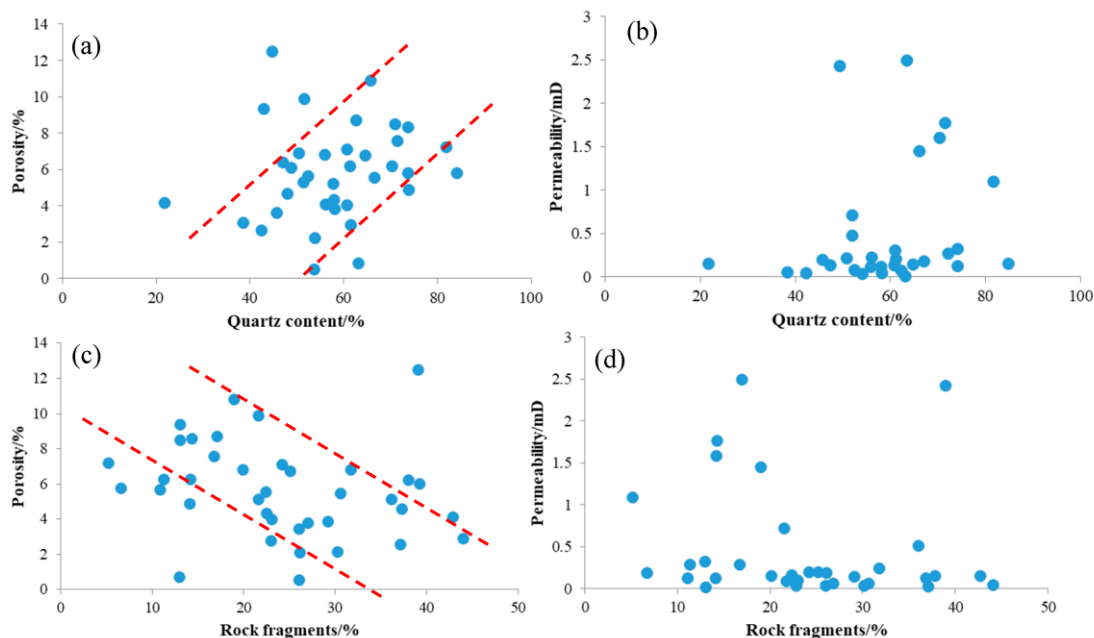


**Figure 11.** The relationship between the quartz content, the rock fragment content, the porosity, and the permeability of the sandstone samples in the study area: (a) The relationship between the quartz content and porosity, and the red dotted lines indicate a positive trend. (b) The relationship between the quartz content and permeability. (c) The relationship between the rock fragment content and porosity, and the red dotted lines indicate a negative trend. (d) The relationship between the rock fragment content and permeability.

## 5.2. Diagenetic Controls on Reservoir Quality

### 5.2.1. Diagenesis Type

**Compaction:** the pressure that is exerted by the overlying strata on the target layer increases as the burial depth increases. This causes intensified compaction [27,28]. The particles primarily experience linear and concave–convex contact during compaction, causing a significant reduction in the pore content and a deterioration in the reservoir quality. Compaction can decrease the porosity of sandstone reservoirs by over 50% and shale gas reservoirs by approximately 70% [29]. In the study area, sandstone reservoirs with favorable porosity and permeability are predominantly found in the relatively shallow-buried Shiqianfeng Formation and Shihezi Formation. The porosity of the sandstone in the study area generally decreases with increasing burial depth, while there is no significant correlation between the permeability and burial depth (Figure 12), indicating that compaction affects porosity. Even though there is a correlation between burial depth and porosity, the data points also exhibit variability, suggesting that the intensity of compaction is influenced by factors such as sandstone composition and other factors such as cementation. A sandstone that is predominantly composed of rigid particles like quartz may exhibit less compaction even at greater burial depths, indicating the effect of composition on compaction and porosity [26].

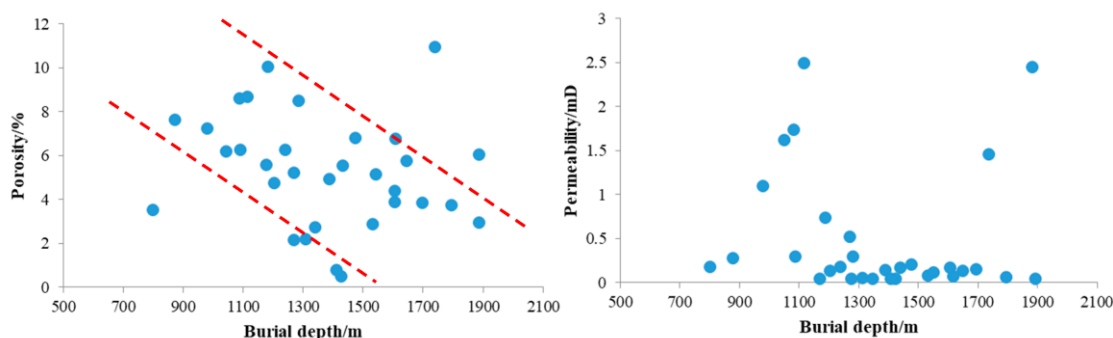


**Figure 12.** The relationship between burial depth and the porosity and permeability of sandstone reservoirs. The red dotted lines indicate a negative trend.

**Cementation:** the main types of cementation in the study area include clay mineral cementation, siliceous cementation, and calcite cementation (Figure 13). Illite, which forms during the middle-late diagenetic stage, is a common clay mineral that occurs in the rocks from the study area. It primarily occurs in hair-like, needle-like, and fibrous forms, where it coats other particles. Kaolinite occurs predominantly as plate-like, book-like, or vermicular structures. Plate-like kaolinite forms due to feldspar dissolution in acidic water bodies during the early diagenetic stage. Kaolinite, which exhibits well-developed crystal forms, primarily fills the dissolution pores or intergranular pores and is mainly formed during the late diagenetic stage. Similar to illite, chlorite partially fills the pores. Siliceous cementation in sandstone reservoirs commonly appears in two forms: quartz overgrowth and microcrystalline quartz aggregates (Figure 13e,f). Calcite cementation is also prevalent in the Shihezi Formation. During the early diagenetic stage, microcrystalline calcite primarily grows in a ctenoid form around clastic particles. During the late diagenetic stage, it is susceptible to replacement by carbonate cement (Figure 13d). Late-stage calcite cement typically forms during intense compaction in the late diagenetic stage.

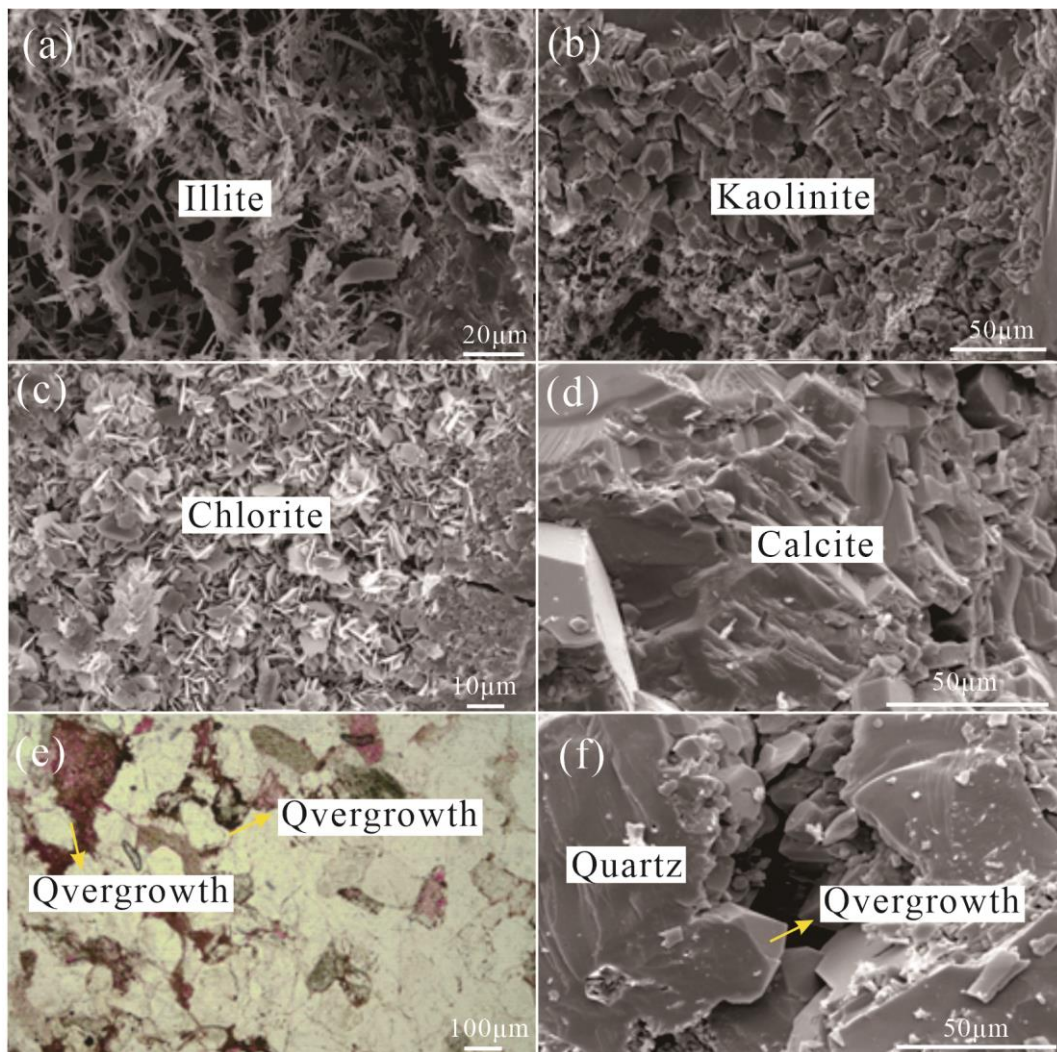


**Figure 13.** The occurrence and characteristics of cement observed under optical microscopy and SEM: (a) lamellar and hair-like authigenic illite; (b) book-like kaolinite aggregate; (c) needle-like chlorite aggregate; (d) authigenic calcite; (e,f) quartz overgrowth.

Cementation can occur during all the stages of diagenesis. Since the cement mainly fills the pores, a higher cement content usually leads to poorer reservoir properties [30,31]. The cements identified in the study area rocks mainly include authigenic clay minerals such as kaolinite, carbonate minerals such as calcite and dolomite, and siliceous minerals such as quartz overgrowth. The carbonate mineral content shows a negative correlation with porosity; as the carbonate mineral content increases, porosity decreases (Figure 14a). Even though carbonate cement can be partially dissolved to form dissolution pores in an acidic environment, the overall correlation between the carbonate mineral content and the reservoir's physical parameters is negative, indicating relatively underdeveloped dissolution pores. There is no significant correlation between the clay mineral content and the porosity and permeability (Figure 14c,d). Kaolinite, illite, and chlorite have high plasticity and are susceptible to compaction, causing a reduction in the primary pores. The intercrystalline pores of these clays are, however, well developed, and the micropores within the clay mineral aggregates are easily preserved [32]. The influence of clay minerals on reservoir properties is relatively complex and can have both positive and negative effects.

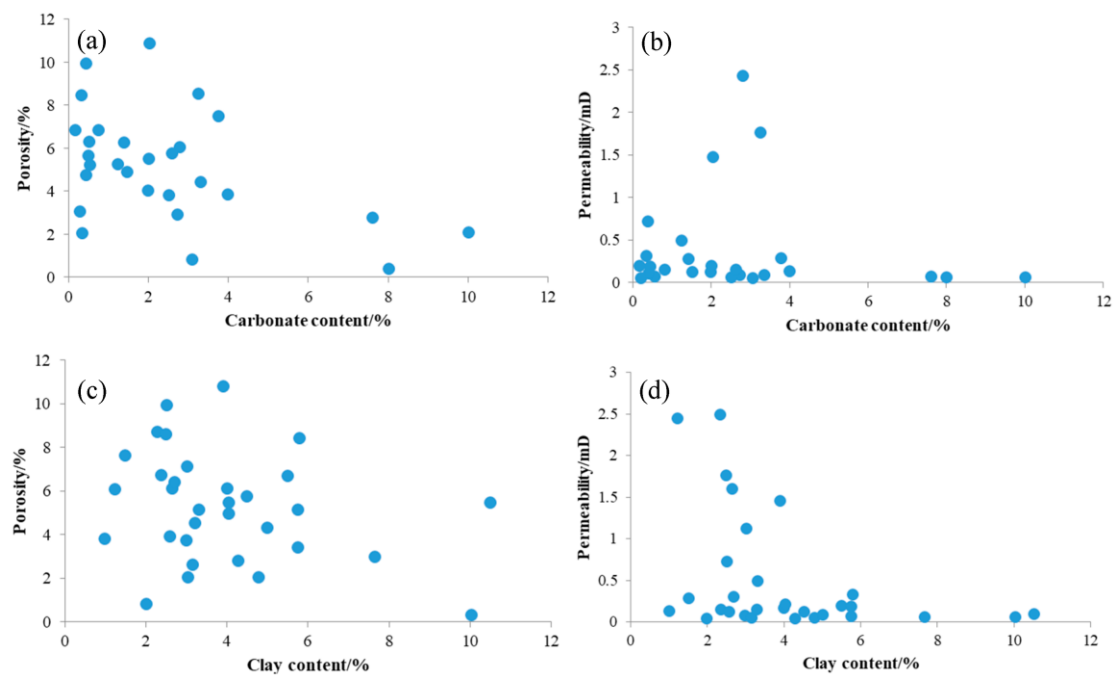


**Figure 14.** The relationship between the cement content and the porosity and permeability of the sandstone hydrocarbon reservoirs: (a) The relationship between the carbonate content and the porosity, (b) the relationship between the carbonate content and the permeability, (c) the relationship between the clay content and the porosity, and (d) the relationship between the clay content and the permeability.

**Dissolution:** dissolution is a constructive diagenetic process that can enhance the physical properties of hydrocarbon reservoirs. Chemically unstable debris particles, cement, and matrices can undergo dissolution under specific conditions, causing the development of secondary pores [33]. The sandstone reservoirs in the study area experienced varying degrees of dissolution (Figure 9a–d). The thermal maturity of source rocks increases as the burial depth increases, causing the production of organic acids during hydrocarbon generation. These acidic fluids can infiltrate the sandstone reservoir, causing the dissolution of feldspar and carbonate minerals. The resulting dissolution of pores can significantly enhance the pore connectivity of the reservoir [34,35]. When the carbonate mineral content is less than 2% (Figure 14a,b), certain sandstone samples exhibit high porosity and permeability, which could be attributed to the dominant role that dissolution and limited cementation play in improving the reservoir quality.

### 5.2.2. Influence of the Diagenesis Type on the Porosity

The physical properties of sandstone reservoirs in the study area are influenced by both destructive diagenesis, such as compaction and cementation, and constructive diagenesis, namely dissolution. To quantify these processes, the pore evolution was calculated using a quantitative method [36,37]. The porosity loss resulting from compaction and cementation during the burial of sandstone reservoirs in the Taiyuan, Shanxi, Shihezi, and Shiqianfeng formations in the Shilouan area was calculated, along with the porosity increase caused by dissolution.

The initial porosity can be determined using the following equations, which are based on the relationship between the initial porosity and sorting coefficient of sandstone reservoirs as proposed by Beard and Weyl (1973) [36]:

$$\varphi_1 = 20.91 + 22.90/S_0 \quad (1)$$

$$S_0 = (d_{75}/d_{25})^{1/2}, \quad (2)$$

where  $\varphi_1$  represents the initial porosity in %;  $S_0$  denotes the sorting coefficient;  $d_{75}$  is the particle diameter in the cumulative curve corresponding to 75% cumulative content; and  $d_{25}$  represents the particle diameter in the cumulative curve corresponding to 25% cumulative content. The value of  $d_{75}$  and  $d_{25}$  were obtained through particle size analysis experiments.

The formulae for calculating the porosity loss caused by compaction and cementation, as well as the porosity increase caused by dissolution, are as follows [38]:

$$\varphi_2 = C + (P_1 \times P_0/P_t) \quad (3)$$

$$\varphi_3 = P_1 \times P_0/P_t \quad (4)$$

$$\varphi_4 = P_2 \times P_0/P_t, \quad (5)$$

where  $\varphi_2$  represents the porosity reduced by compaction in %;  $\varphi_3$  denotes the porosity reduced by cementation in %;  $\varphi_4$  is the porosity increased by dissolution in %;  $C$  represents the cement content in %;  $P_0$  denotes the measured porosity in %;  $P_1$  is the intergranular porosity in %;  $P_2$  represents the dissolution porosity in %; and  $P_t$  denotes the total porosity in %. The values of  $C$ ,  $P_1$ ,  $P_t$ , and  $P_2$  were obtained through observation and statistical analysis of cast thin sections.

The primary porosity in the study area exhibits a relatively narrow range, varying from 31.3% to 38.9% (Figure 15), which is comparable to the predominant tight sandstone gas formations in the Ordos Basin. Compaction and cementation have notably reduced the porosity, with compaction accounting for a porosity decrease ranging from 22% to 28.9%, while cementation contributed to a porosity decrease ranging from 5.7% to 7.2%. The Xiashihezi Formation shows the smallest porosity decrease due to compaction, while the Shanxi Formation exhibits the largest porosity decrease due to compaction, and the Benxi Formation shows the largest porosity decrease due to cementation. Compaction primarily causes a reduction in porosity, accounting for over 70% of the porosity decrease. Dissolution has also positively affected the physical properties of the reservoir, causing a porosity increase ranging between 2.9% and 4.8%. The Shangshihezi Formation exhibits the most developed dissolution process and the highest porosity.

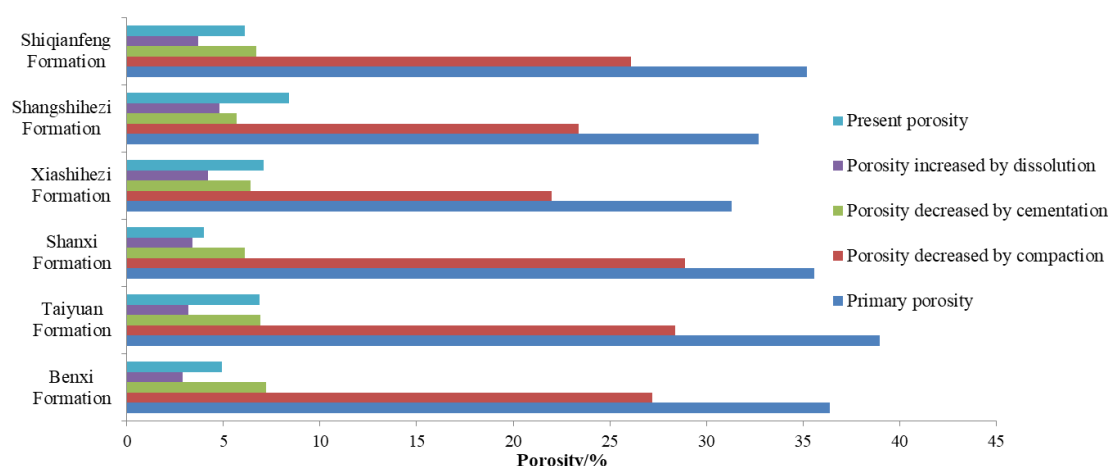


**Figure 15.** Statistical analysis of the quantitative parameters for the porosity evolution in the Carboniferous–Permian sedimentary succession from the study area.

As the sediments experience an increasing burial depth during the early diagenetic stage, compaction becomes the dominant diagenetic process. This caused the closure of numerous primary intergranular pores, causing a rapid decrease in porosity. During the early diagenetic stage, porosity reduction due to compaction can be as high as 20%. As the

burial depth continues to increase during the later stages of diagenesis, porosity reduction due to compaction is around 10%. The gradual rise in the formation temperature also causes the generation of authigenic minerals like quartz, kaolinite, and illite. These minerals further fill the pore spaces and consequently decrease porosity. The Carboniferous–Permian coal measures are characterized by the widespread development of source rocks, including coal and black shale. The abundant organic matter in these rocks produced organic acid as it underwent hydrocarbon generation [32]. These acids dissolve feldspar, rock fragments, and other minerals, thereby improving the physical properties of the hydrocarbon reservoir and increasing the porosity by approximately 5%. The Carboniferous–Permian strata experienced gradual uplift in the study area during the late diagenetic stage, and the occurrence of micro-cracks due to tectonic processes was relatively limited. The sandstone reservoirs in the study area, therefore, exhibit tight characteristics (Figure 16).

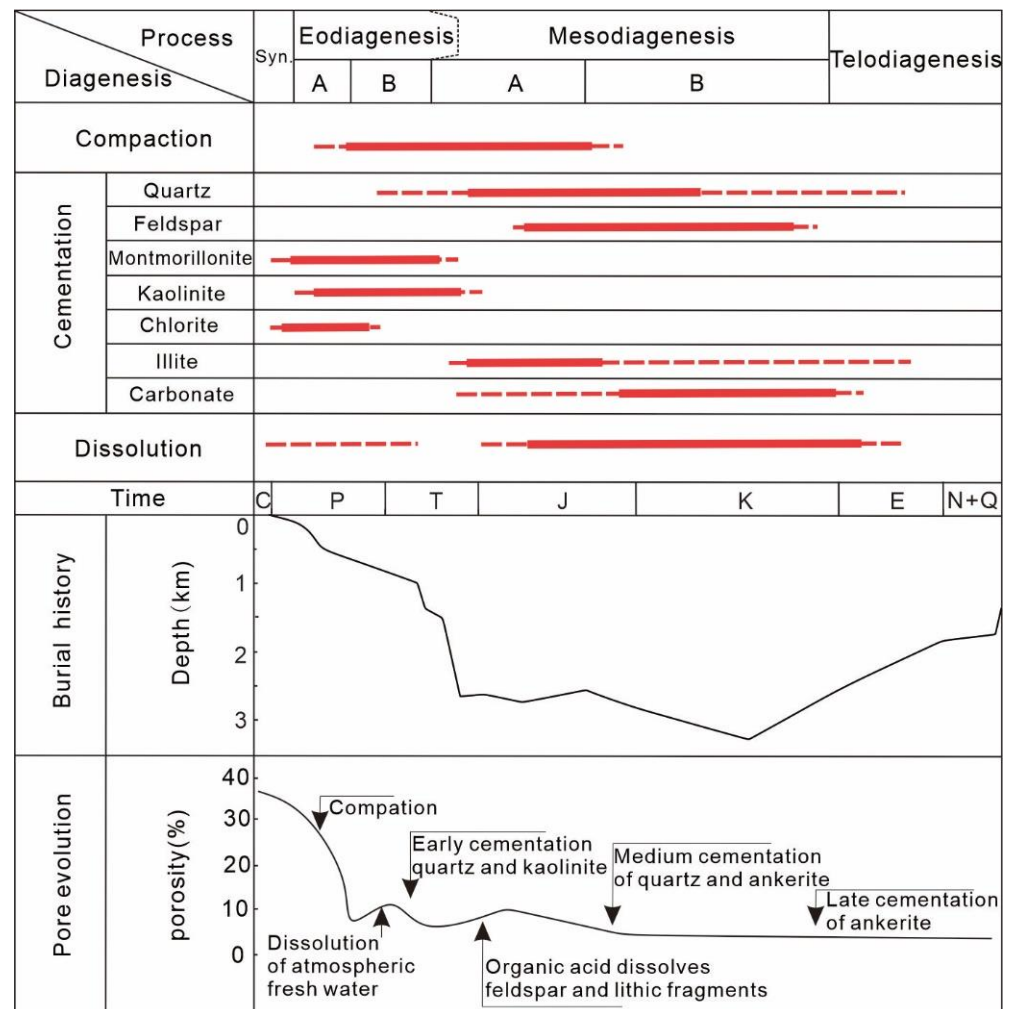
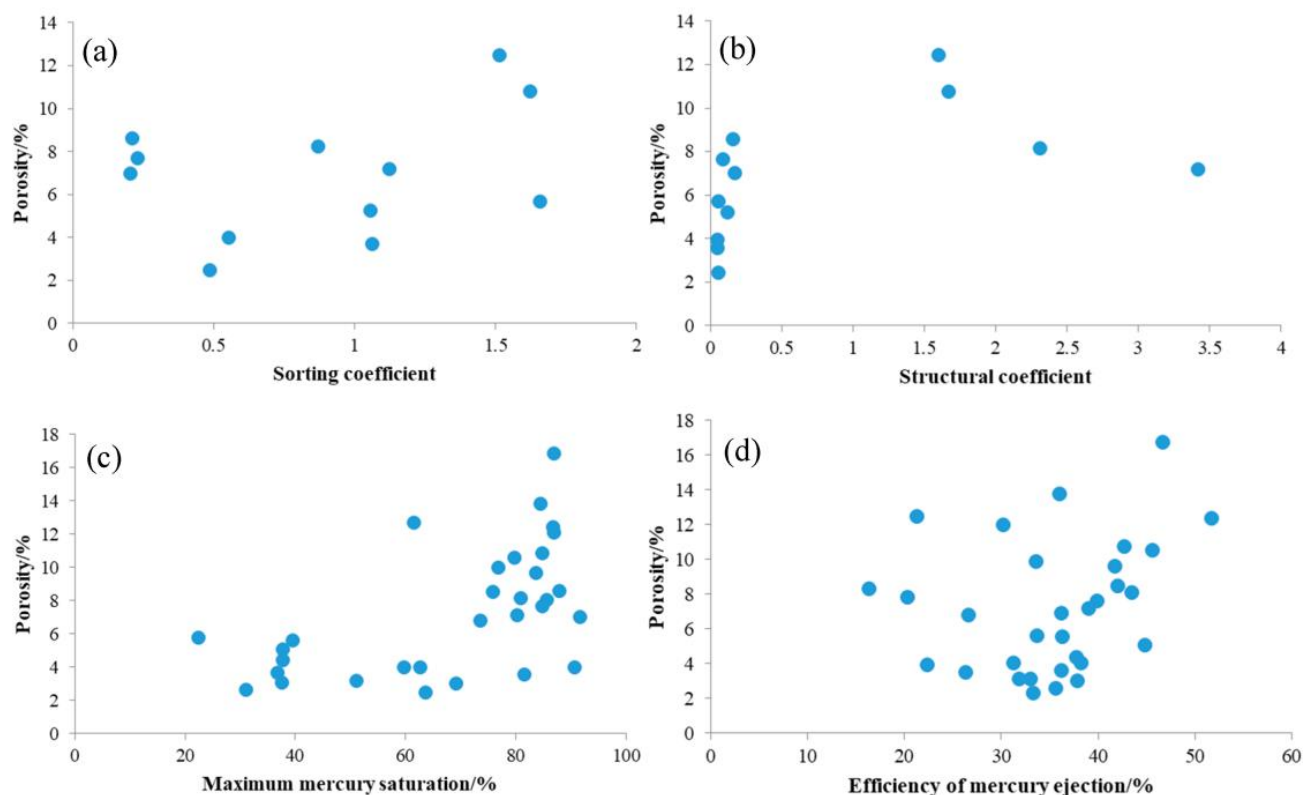


Figure 16. Diagenetic evolution of sandstone reservoirs in the study area and its effect on porosity.

### 5.3. Pore Structure Controls on the Reservoir Quality

Using mercury intrusion experiments, various parameters reflecting pore structure characteristics were obtained (Table 2). There is a weak positive correlation between the porosity and the sorting coefficient, indicating that porosity tends to increase with an increase in the sorting coefficient (Figure 17a). SEM and cast thin section analyses revealed that the Shihezi Formation has relatively well-developed pores, with intergranular pores and dissolution pores being the main type. These dissolution pores exhibit diverse morphologies, and the pore throat sizes have an uneven distribution. Samples with higher sorting coefficients tend to have larger pore sizes and smaller throats. Sandstone reservoirs

with larger pores have higher permeability, while micro throats facilitate gas occurrence and storage [39,40].



**Figure 17.** Relationship between the pore structure parameters and the porosity of the sandstone reservoirs in the study area: (a) The relationship between the sorting coefficient and the porosity, (b) the relationship between the structural coefficient and the porosity, (c) the relationship between the maximum mercury saturation and the porosity, and (d) the relationship between the efficiency of mercury ejection and the porosity.

Unlike the sorting coefficient, there is no significant correlation between the structural coefficient and the porosity (Figure 17b), suggesting that the tortuosity of the pore throat has a minimal impact on porosity. There may, however, be a distinct relationship between the structural coefficient and permeability. Higher tortuosities in the pore throat generally make seepage more challenging. The parameters related to mercury saturation include maximum mercury saturation and efficiency of mercury ejection. There is a positive correlation between the maximum mercury saturation and the porosity, while the efficiency of mercury ejection shows no significant correlation with porosity (Figure 17c,d). This means that the pore structure is favorable for the accumulation of sandstone gas but not for gas seepage.

#### 5.4. Evaluation of Sandstone Reservoirs

Within the Carboniferous–Permian sedimentary succession, the characteristics of sandstone reservoirs in the study area vary significantly. The sandstone reservoirs in the Shilounan Block were classified into three types based on factors such as sedimentary facies, sandstone distribution, physical properties, and the influence of sedimentation, diagenesis, and pore structure on reservoir quality [41–43] (Table 4):

Type I: the type I reservoir is predominantly found in the primary areas of the superimposed multiphase distributary channels within the study area. The type I sandstone reservoir exhibits relatively high porosity and permeability, with quartz sandstone being the primary lithology [44]. The grain size of the type I reservoir ranges from medium to

coarse and displays good sorting. The main types of cement are siliceous minerals and kaolinite. The pore structure of the type I reservoirs consists of a combination of dissolution pores and residual intergranular pores. The pore structure characteristics are relatively straightforward, with a displacement pressure that is typically below 1 MPa and an average throat radius of 0.4  $\mu\text{m}$ . Type I reservoirs, which are mainly developed in the Shihezi Formation, should be considered as a primary focus for future hydrocarbon exploration and development efforts.

Type II: the type II reservoir occurs in the principal sand bodies of the subaqueous distributary channels. The rock particle size ranges from medium to fine, with an increased presence of interstitial materials. Compaction and cementation are more pronounced in the type II reservoirs compared to the type I reservoirs, causing a significant reduction in the primary intergranular pores. The porosity generally ranges between 5% and 10%, with a moderate displacement pressure. The pore development of the type II reservoirs is noticeably lower compared to the type I reservoirs. The predominant pore types are intergranular pores and intercrystalline pores, with an average throat size of 0.2 to 0.4  $\mu\text{m}$ . This type of reservoir can serve as an alternative target for exploration and development within the Shilounan Block [45,46]. The type II reservoir is primarily developed in the Shiqianfeng Formation.

Type III: the type III reservoir is mainly developed in the underwater distributary channels and consists predominantly of fine-grained lithic sandstones, siltstones, and argillaceous siltstones. This reservoir exhibits relatively compact characteristics. It has a high presence of interstitial material, and compaction and cementation significantly affect the reservoir properties [47,48]. The particles often exhibit concave–convex and mosaic-like contacts, which causes a substantial reduction in the primary pores and limited development of the secondary dissolution pores. The porosity typically falls below 5%. The predominant pore type is intercrystalline pores, with an average throat size of less than 0.2  $\mu\text{m}$ . The displacement pressure of type III reservoirs is relatively high, and larger-sized pores and fractures are generally scarce. The type III reservoirs are primarily developed in the Shanxi Formation and the Taiyuan Formation.

**Table 4.** Comprehensive evaluation parameters for sandstone reservoirs in the study area.

	Parameters	Type I	Type II	Type III
Depositional Feature	Single-layer sandstone thickness/m	>8	3–8	3<
	Sandstone type	Coarse- to medium-grained quartz sandstone, lithic quartz sandstone, with low interstitial content	Medium- to fine-grained quartz lithic sandstone, lithic sandstone, medium to low interstitial content, kaolinite is the predominant clay mineral	Fine-grained lithic sandstone, with high content of fillings, mainly carbonates and clay minerals
	Sand body type	Channel sand body	Channel sand body, underwater distributary channel sands	Underwater distributary channel sands
Physical Property	Porosity/%	>10	5–10	5<
	Permeability/mD	>0.5	0.1–0.6	0.1<
Pore Structure	Pore type	Intergranular and dissolution pores	Intergranular and dissolution pores	Intercrystalline pores
	Pore-Throat	Mesopore-fine throat, moderately sorted	Fine-micro throat, poorly sorted	Micro-throat, poorly sorted
	Displacement pressure	Low	Medium	High
	Average throat size/ $\mu\text{m}$	>0.4	0.2–0.4	0.2<
Reservoir Properties		High quality	Good	Average and lower

## 6. Conclusions

(1) The predominant sandstone type in the Shilounan Block is lithic sandstone, which has a low porosity and ultra-low permeability reservoir. The primary types of pores present are intergranular pores, intercrystalline pores, and dissolution pores. The Shihezi Formation exhibits relatively good porosity and pore connectivity, characterized by a larger average throat size. In contrast, the Taiyuan and Shanxi formations have poor pore connectivity and have smaller throats.

(2) The primary controlling factors influencing the sandstone reservoirs in the study area are diagenesis and sedimentation. Sedimentation determines the distribution characteristics of the sand bodies and their petrological features, including the composition and grain size. Compaction and cementation caused the loss of a significant number of primary pores, leading to unfavorable reservoir properties. Compaction has notably reduced the porosity, accounting for over 70% of the overall porosity decrease. Dissolution processes have been relatively limited in the Shilounan Block, contributing to the relatively tight nature of the reservoirs in this region.

(3) A comprehensive evaluation system has been established to assess tight sandstone reservoirs in the Shilounan Block. This system is based on sedimentary characteristics such as sandstone thickness, sandstone type, and sand body type, while the primary discriminant criteria are porosity, permeability, and pore structure parameters. Using this evaluation system, it is determined that the high-quality reservoirs in the study area are primarily developed in the Shihezi Formation.

**Author Contributions:** Methodology, J.W.; writing—original draft preparation, J.W., F.Y. and Z.X.; writing—review and editing, J.W., F.Y. and C.Z. All authors have read and agreed to the published version of the manuscript.

**Funding:** This research received no external funding.

**Data Availability Statement:** Data is unavailable due to privacy or ethical restrictions.

**Acknowledgments:** The authors would like to thank Fundamental Research Funds for the Central Universities (grant no. 2652019106). We also thank the editors and reviewers very much for their critical comments and valuable suggestions, which were very helpful in improving the manuscript.

**Conflicts of Interest:** The authors declare no conflict of interest.

## References

1. Nelson, P.H. Pore-throat sizes in sandstones, tight sandstones, and shales. *AAPG Bull.* **2009**, *93*, 329–340. [[CrossRef](#)]
2. Zou, C.N.; Zhu, R.K.; Wu, S.T.; Yang, Z.; Tao, S.Z.; Yuan, X.J.; Hou, L.H.; Yang, H.; Xu, C.C.; Li, D.H.; et al. Types, characteristics, genesis and prospects of conventional and unconventional hydrocarbon accumulations: Taking tight oil and tight gas in China as an instance. *Acta Pet. Sin.* **2012**, *33*, 173–187.
3. Nabawy, B.S.; Abd El Aziz, E.A.; Ramadan, M.; Shehata, A.A. Implication of the micro- and lithofacies types on the quality of a gas-bearing deltaic reservoir in the Nile Delta, Egypt. *Sci. Rep.* **2023**, *13*, 8873. [[CrossRef](#)] [[PubMed](#)]
4. Zou, C.N.; Yang, Z.; Tao, S.Z.; Yuan, X.J.; Zhu, R.K.; Hou, L.H.; Pang, Z.L. Continuous hydrocarbon accumulation over a large area as a distinguishing characteristic of unconventional petroleum: The Ordos Basin, North-Central China. *Earth Sci. Rev.* **2013**, *126*, 358–369. [[CrossRef](#)]
5. Qu, X.; Sun, W.; Lei, Q.; Huang, H.; Huo, L. Study on saturation of movable fluid in the low-permeability sandstone reservoirs of Huaqing Oilfield and its influencing factors. *J. Xi'an Shiyou Univ. (Nat. Sci. Ed.)* **2016**, *31*, 93–98.
6. Liu, M.J.; Xiong, C. Diagenesis and reservoir quality of deep-lacustrine sandy-debris-flow tight sandstones in Upper Triassic Yanchang Formation, Ordos Basin, China: Implications for reservoir heterogeneity and hydrocarbon accumulation. *J. Pet. Sci. Eng.* **2021**, *202*, 108548. [[CrossRef](#)]
7. Yang, H.; Fu, J.H.; Liu, X.S.; Meng, P.L. Accumulation conditions and exploration and development of tight gas in the Upper Paleozoic of the Ordos Basin. *Pet. Explor. Dev.* **2012**, *39*, 295–303. [[CrossRef](#)]
8. Schmid, S.; Worden, R.H.; Fisher, Q.J. Diagenesis and reservoir quality of the sherrwood sandstone (triassic), corrib feld, slyne basin, west of Ireland. *Mar. Pet. Geol.* **2004**, *21*, 299–315. [[CrossRef](#)]
9. Lai, J.; Wang, G.; Ran, Y.; Zhou, Z.; Cui, Y. Impact of diagenesis on the reservoir quality of tight oil sandstones: The case of Upper Triassic Yanchang Formation Chang 7 oil layers in Ordos Basin, China. *J. Pet. Sci. Eng.* **2016**, *145*, 54–65. [[CrossRef](#)]

10. Abdel-Fattah, M.I.; Sen, S.; Abuzied, S.M.; Abioui, M.; Radwan, A.E.; Benssaou, M. Facies analysis and petrophysical investigation of the late miocene abu madi sandstones gas reservoirs from offshore baltim east field (nile delta, Egypt). *Mar. Pet. Geol.* **2022**, *137*, 105501. [[CrossRef](#)]
11. Radwan, A.E.; Husinec, A.; Benjumea, B.; Kassem, A.A.; Abd El Aal, A.K.; Hakimi, M.H.; Thanh, H.V.; Abdel-Fattah, M.I.; Shehata, A.A. Diagenetic overprint on porosity and permeability of a combined conventional-unconventional reservoir: Insights from the Eocene pelagic limestones, Gulf of Suez, Egypt. *Mar. Pet. Geol.* **2022**, *146*, 105967.
12. Dong, S.; Zeng, L.; Lyu, W.; Xia, D.; Liu, G.; Wu, Y.; Du, X. Fracture identification and evaluation using conventional logs in tight sandstones: A case study in the Ordos Basin, China. *Energy Geosci.* **2020**, *1*, 115–123. [[CrossRef](#)]
13. Wei, J.X.; Chen, S.; Gu, Y.; Zhang, H.; Yin, S.; Yuan, H. Diagenesis and reservoir classification criteria for Jurassic continental sandstone oil reservoir in the western Ordos Basin, China. *Geol. J.* **2021**, *56*, 3868–3882. [[CrossRef](#)]
14. Zhao, Z.; Liu, Z.; He, F.Q.; Zhang, W.; Li, M.; Hou, Y.J.; Fu, S.; Zhu, M.L. An improved time–depth dual porosity evolution model and a new parameter for tight sandstone reservoir quality evaluation. *J. Asian Earth Sci.* **2023**, *252*, 105684. [[CrossRef](#)]
15. Tang, S.L.; Tang, D.Z.; Liu, S.M.; Li, S.; Tang, J.C.; Wang, M.F.; Zhang, A.B.; Pu, Y.F. Multiscale pore characterization of coal measure reservoirs and gas storage and transport behavior in Yanchuannan gas field of China. *AAPG Bull.* **2022**, *106*, 2387–2415. [[CrossRef](#)]
16. Zhang, A.B.; Chen, S.D.; Tang, D.Z.; Tang, S.L.; Zhang, T.Y.; Pu, Y.F.; Sun, B. The Study on Diagenetic Characteristics of Coal Measures Sandstone Reservoir in Xishanyao Formation, Southern Margin of the Junggar Basin. *Energies* **2022**, *15*, 5499. [[CrossRef](#)]
17. Worden, R.H.; Mayall, M.; Evans, I.J. The effect of ductile-lithic sand grains and quartz cement on porosity and permeability in Oligocene and lower Miocene clastics, South China Sea: Prediction of reservoir quality. *Am. Assoc. Pet. Geol. Bull.* **2000**, *84*, 345–359.
18. Liu, K.; Wang, R.; Shi, W.Z.; Travéb, A.; Martín-Martín, J.D.; Baqués, V.; Qi, R.; Lin, J.W.; Ye, H. Diagenetic controls on reservoir quality and heterogeneity of the Triassic Chang 8 tight sandstones in the Binchang area (Ordos Basin, China). *Mar. Pet. Geol.* **2022**, *146*, 105974. [[CrossRef](#)]
19. Cai, Y. Study on the Relationship between Reservoir Evolution and Oil Accumulation Process of Chang 8 Tight Sandstone Oil Reservoir in Jiyuan Area, Ordos Basin. Ph.D. Thesis, Chang’an University, Xi’an, China, 2015.
20. Liang, J.T.; Huang, W.H.; Wang, H.L.; Blum, M.J.; Chen, J.; Wei, X.L.; Yang, G.Q. Organic geochemical and petrophysical characteristics of transitional coalmeasure shale gas reservoirs and their relationships with sedimentary environments: A case study from the Carboniferous-Permian Qinshui Basin, China. *J. Pet. Sci. Eng.* **2020**, *184*, 106510. [[CrossRef](#)]
21. Mansurbeg, H.; De Ros, L.F.; Morad, S.; Ketzer, J.M.; El-Ghali, M.A.K.; Caja, M.A.; Othman, R. Meteoric-water diagenesis in late Cretaceous canyon-fill turbidite reservoirs from the Espirito Santo Basin, eastern Brazil. *Mar. Pet. Geol.* **2012**, *37*, 7–26. [[CrossRef](#)]
22. Yang, T.; Cao, Y.; Friis, H.; Liu, K.; Wang, Y.; Zhou, L.; Yuan, G.; Xi, K.; Zhang, S. Diagenesis and reservoir quality of lacustrine deep-water gravity-flow sandstones in the Eocene Shahejie Formation in the Dongying sag, Jiyang depression, eastern China. *AAPG Bull.* **2020**, *104*, 1045–1073. [[CrossRef](#)]
23. Zhou, X.; He, Y.; Wang, J.; Li, S.; Ling, A. Characteristics of sandy debris flow reservoir from Chang 6 Formation in Ordos Basin. *Sci. Technol. Eng.* **2014**, *14*, 216–220. (In Chinese with English Abstract).
24. Liao, J.; Xi, A.; Li, Z.; Liu, H.; Li, X.; Wanyan, R. Microscopic characterization and formation mechanisms of deepwater sandy-debris-flow and turbidity-current sandstones in a lacustrine basin: A case study in the Yanchang Formation of the Ordos Basin, China. *Pet. Sci.* **2018**, *15*, 28–40. [[CrossRef](#)]
25. Xi, Z.D.; Tang, S.H.; Li, J.; Zhang, Z.Y.; Xiao, H.Q. Pore characterization and the controls of organic matter and quartz on pore structure: Case study of the Niutitang Formation of northern Guizhou Province, South China. *J. Nat. Gas Sci. Eng.* **2019**, *61*, 18–31. [[CrossRef](#)]
26. Xi, Z.D.; Tang, S.H.; Lash, G.G.; Ye, Y.P.; Lin, D.L.; Zhang, B. Depositional controlling factors on pore distribution and structure in the lower Silurian Longmaxi shales: Insight from geochemistry and petrology. *Mar. Pet. Geol.* **2021**, *130*, 105114. [[CrossRef](#)]
27. Lundegard, P.D. Sandstone porosity loss—a “big picture” view of the importance of compaction. *J. Sediment. Res.* **1992**, *62*, 250–260. [[CrossRef](#)]
28. Paxton, S.T.; Szabo, J.O.; Ajdukiewicz, J.M.; Klimentidis, R.E. Construction of an intergranular volume compaction curve for evaluating and predicting compaction and porosity loss in rigid-grain sandstone reservoirs. *Am. Assoc. Pet. Geol.* **2002**, *86*, 2047–2067.
29. Ehrenberg, S.N. Assessing the relative importance of compaction processes and cementation to reduction of porosity in sandstones: Discussion; compaction and porosity evolution of Pliocene sandstones, Ventura basin, California: Discussion. *AAPG Bull.* **1989**, *73*, 1274–1276.
30. Taylor, K.G.; Gawthorpe, R.L.; Curtis, C.D.; Marshall, J.D.; Awwiller, D.N. Carbonate cementation in a sequence-stratigraphic framework: Upper Cretaceous sandstones, Book Cliffs, Utah-Colorado. *J. Sediment. Res.* **2000**, *70*, 360–372. [[CrossRef](#)]
31. Dutton, S.P. Calcite cement in Permian deep-water sandstones, Delaware Basin, west Texas: Origin, distribution, and effect on reservoir properties. *AAPG Bull.* **2008**, *92*, 765–787. [[CrossRef](#)]
32. Xi, Z.D.; Tang, S.H.; Wang, J.; Yang, G.Q.; Li, L. Formation and development of pore structure in marine-continental transitional shale from northern China across a maturation gradient: Insights from gas adsorption and mercury intrusion. *Int. J. Coal Geol.* **2018**, *200*, 87–102. [[CrossRef](#)]

33. Ma, B.; Cao, Y.; Jia, Y. Feldspar dissolution with implications for reservoir quality in tight gas sandstones: Evidence from the Eocene Es4 interval, Dongying Depression, Bohai Bay Basin, China. *J. Pet. Sci. Eng.* **2017**, *150*, 74–84. [[CrossRef](#)]
34. Mahmi, O.; Dypvik, H.; Hammer, E. Diagenetic influence on reservoir quality evolution, examples from Triassic conglomerates/arenites in the Edvard Grieg field, Norwegian North Sea. *Mar. Pet. Geol.* **2018**, *93*, 247–271. [[CrossRef](#)]
35. Zhang, Y.; Jiang, S.; He, Z.; Wang, Y.; Chen, G. Characteristics of heterogeneous diagenesis and modification to physical properties of Upper Paleozoic tight gas reservoir in eastern Ordos Basin. *J. Pet. Sci. Eng.* **2022**, *208*, 109243. [[CrossRef](#)]
36. Beard, D.C.; Weyl, P.K. Influence of texture on porosity and permeability of unconsolidated sand. *AAPG Bull.* **1973**, *57*, 349–369.
37. Yang, J.Q.; Ji, Y.L.; Wu, H.; Meng, L.J. Diagenesis and Porosity Evolution of Deep Reservoirs in the Nanpu Sag: A case study of Sha 1 Member of the Paleogene in No. 3 structural belt. *Acta Sedimentol. Sin.* **2022**, *40*, 203–216.
38. Wilson, J.C.; McBride, E.F. Compaction and porosity evolution of Pliocene sandstones, Ventura Basin, California. *AAPG Bull.* **1989**, *73*, 664–681.
39. Wang, R.; Shi, W.; Xie, X.; Zhang, W.; Qin, S.; Liu, K.; Busbey Arthur, B. Clay mineral content, type, and their effects on pore throat structure and reservoir properties: Insight from the Permian tight sandstones in the Hangjinqi area, north Ordos Basin, China. *Mar. Pet. Geol.* **2020**, *115*, 104281. [[CrossRef](#)]
40. Law, B.E. Basin-centered gas systems. *AAPG Bull.* **2002**, *86*, 1891–1919.
41. Bell, D.; Kane, I.A.; Pontén, A.S.M.; Flint, S.S.; Hodgson, D.M.; Barrett, B.J. Spatial variability in depositional reservoir quality of deep-water channel-fill and lobe deposits. *Mar. Pet. Geol.* **2018**, *98*, 97–115. [[CrossRef](#)]
42. Fic, J.; Pedersen, P.K. Reservoir characterization of a “tight” oil reservoir, the middle jurassic upper shaunavon member in the whitemud and eastbrook pools, SW saskatchewan. *Mar. Pet. Geol.* **2013**, *44*, 41–59. [[CrossRef](#)]
43. Liu, D.; Sun, W.; Ren, D.; Li, C. Quartz cement origins and impact on storage performance in Permian Upper Shihezi Formation tight sandstone reservoirs in the northern Ordos Basin, China. *J. Pet. Sci. Eng.* **2019**, *178*, 485–496. [[CrossRef](#)]
44. Ghanizadeh, G.; Clarkson, C.R.; Aquino, S.; Ardakani, O.H.; Sane, H. Petrophysical and geomechanical characteristics of Canadian tight oil and liquid-rich gas reservoirs: I. Pore network and permeability characterization. *Fuel* **2015**, *153*, 664–681. [[CrossRef](#)]
45. Li, Z.; Wu, S.; Xia, D.; He, S.; Zhang, X. An investigation into pore structure and petrophysical property in tight sandstones: A case of the Yanchang Formation in the southern Ordos Basin, China. *Mar. Pet. Geol.* **2018**, *97*, 390–406. [[CrossRef](#)]
46. Sakhaee-Pour, A.; Bryant, S.L. Effect of pore structure on the producibility of tightgas sandstones. *AAPG Bull.* **2014**, *98*, 663–694. [[CrossRef](#)]
47. Christopher, B.; Kuiwu, L.; Oswald, G. Diagenesis and reservoir properties of the permian ecca group sandstones and mudrocks in the eastern cape province, South Africa. *Minerals* **2017**, *7*, 88.
48. Enayati-Bidgoli, A.; Saemi, E. Effects of late diagenesis on primary reservoir quality of a quartz arenite unit: A case study from the lower Cretaceous successions of SW Iran. *Pet. Sci.* **2019**, *16*, 267–284. [[CrossRef](#)]

**Disclaimer/Publisher’s Note:** The statements, opinions and data contained in all publications are solely those of the individual author(s) and contributor(s) and not of MDPI and/or the editor(s). MDPI and/or the editor(s) disclaim responsibility for any injury to people or property resulting from any ideas, methods, instructions or products referred to in the content.